

## Numerical analysis of a dynamic problem involving bulk-surface surfactants

Marco Campo<sup>1</sup> · José R. Fernández<sup>2</sup>  · María del Carmen Muñiz<sup>3</sup> · Cristina Núñez<sup>4</sup>

Received: 19 May 2017 / Accepted: 22 July 2017 / Published online: 1 August 2017  
© Springer International Publishing AG 2017

**Abstract** In this paper, a dynamic problem which models the evolution of the concentration of surfactants is analyzed from the numerical point of view. Both bulk and surface diffusions are taken into account into the model, and the relationship between both concentrations, in the bulk and at the surface, is considered by using the well-known Langmuir–Hinshelwood equation. Two convective terms are also included. The variational formulation is then written as a coupled system of parabolic partial differential equations, for which an existence and uniqueness result is stated in an earlier paper (Fernández et al. in *SIAM J Math Anal* 48(5):3065–3089, 2016). Then, fully

---

This work has been supported by Ministerio de Economía y Competitividad under the Project MTM2015-66640-P (with the participation of FEDER).

---

✉ José R. Fernández  
jose.fernandez@uvigo.es

Marco Campo  
marco.campo@udc.es

María del Carmen Muñiz  
mcarmen.muniz@usc.es

Cristina Núñez  
cngarcia@unizar.es

- <sup>1</sup> Departamento de Matemáticas, ETS de Ingenieros de Caminos, Canales y Puertos, Universidade da Coruña, Campus de Elviña, 15071 A Coruña, Spain
- <sup>2</sup> Departamento de Matemática Aplicada I, ETSI Telecomunicación, Universidade de Vigo, Campus As Lagoas Marcosende s/n, 36310 Vigo, Spain
- <sup>3</sup> Departamento de Matemática Aplicada, Facultad de Matemáticas, Universidade de Santiago de Compostela, Campus Vida s/n, 15782 Santiago de Compostela, Spain
- <sup>4</sup> Departamento de Matemáticas, Facultad de Ciencias Sociales y Humanas, Universidad de Zaragoza, Ciudad Escolar s/n, 44033 Teruel, Spain

discrete approximations are introduced by using the classical finite element method to approximate the spatial variable and the implicit Euler scheme to discretize the time derivatives. An a priori error estimates result is proved, from which the linear convergence of the approximation is derived under suitable additional regularity conditions. Finally, some numerical simulations are presented in order to show the accuracy of the algorithm and the behaviour of the solution in real situations.

**Keywords** Adsorption dynamic model · Surfactants · Langmuir isotherm · Surface diffusion · A priori error estimates · Numerical simulations

## 1 Introduction

The effect of surfactants is a very important issue in many real world applications, in which the surface tension plays a significant role. For instance, some examples could be the control of the droplet size when forming emulsions, foams, suspensions and pharmaceuticals, the inkjet printing or treatments for decompression illness caused by gas bubbles entering the blood stream during surgery (see, e.g., [19]). In these processes, the new formed surface in the surfactant solution is generated due to the incorporation of molecules, reducing the surface tension, and depending on many features as the salinity, the temperature, the type of surfactant, etc. In this paper, we assume that this process is governed by a mixed kinetic-diffusion model, that is, a kinetic relation between the volumetric and surface concentrations which is written in terms of a parabolic partial differential equation defined on a part of the boundary domain.

In the recent years, some papers have been published dealing with related problems: the linear Henry isotherm [12], the mixed kinetic-diffusion case [13] or the Langmuir–Hinshelwood equation [10]. However, in all these studies a great simplification was assumed, reducing the problem to a one-dimensional version, because we considered the molecules moving in a vertical direction and no diffusion on the surface. Therefore, in this new model, following other authors (see, e.g., [1, 2, 17]), we consider that the problem is either two- or three-dimensional and that there is diffusion of the surface concentration.

Hence, in this paper we continue the research done in [11], where we provided results on the unique weak solvability of the system and nonnegativity of its solution, by using the truncation method combined with the fixed point approach and the theory of time-dependent partial differential equations on manifolds. Our aim now is to introduce fully discrete approximations of the problem, to obtain a priori error estimates and to show some numerical simulations in two and three dimensions.

The paper is outlined as follows. The mathematical model is described in Sect. 2 following [11], deriving its variational formulation. An existence and uniqueness result, proved in [11] is also stated. Then, in Sect. 3 a numerical scheme is introduced, based on the finite element method to approximate the spatial domain and the forward Euler scheme to discretize the time derivatives. A priori error estimates are deduced for the approximative solutions and, under suitable regularity assumptions, the linear

convergence of the algorithm is obtained. Finally, some two- and three-dimensional numerical simulations are presented in Sect. 4.

## 2 Mathematical model

Let  $\Omega$  be an open and bounded domain in  $\mathbb{R}^{d+1}$  with  $d = 1, 2$ . The boundary  $\partial\Omega$  of  $\Omega$  is assumed to be Lipschitz continuous, and it consists of three mutually disjoint parts  $\Gamma_D, \Gamma_N$  and  $\Gamma_S$  such that  $\partial\Omega = \overline{\Gamma_D} \cup \overline{\Gamma_N} \cup \overline{\Gamma_S}$ . We assume that  $\Gamma_D$  and  $\Gamma_S$  have nonzero  $d$ -dimensional Hausdorff measure, and that  $\Gamma_S$  is a compact  $C^\infty$ -Riemannian manifold with a Lipschitz boundary (see p. 166 in [4]). The outward-pointing unit normal vector field  $\boldsymbol{\mu}$  along  $\partial\Gamma_S$  exists almost everywhere with respect to the boundary measure (see the arguments in the Proposition 15.33 of [18] and in the proof of Theorem 11 of [4]).

For a function  $g$ , being defined and smooth in a neighbourhood of  $\Gamma_S$ , the surface (or tangent) gradient on  $\Gamma_S$  is given by

$$\nabla_S g = Dg - (\boldsymbol{\nu} \cdot Dg) \boldsymbol{\nu},$$

where  $Dg(\mathbf{y})$  is the gradient of  $g$  at point  $\mathbf{y}$  and  $\boldsymbol{\nu}$  stands for the outward-pointing unit normal vector along  $\Gamma_S$ . Thus, the surface gradient at a point  $\mathbf{y} \in \Gamma_S$  is the projection of the gradient at  $\mathbf{y}$  onto the tangent plane to  $\Gamma_S$  at  $\mathbf{y}$ . We refer the reader to [14, p. 388], for the definition of hypersurfaces in  $\mathbb{R}^{d+1}$  and surface gradients on them. Furthermore, denoting by  $(\underline{D}_1 g, \dots, \underline{D}_{d+1} g)$  the components of the surface gradient, the Laplace–Beltrami operator is defined by the surface divergence of the surface gradient, that is,

$$\Delta_S g := \nabla_S \cdot \nabla_S g = \sum_{i=1}^{d+1} \underline{D}_i \underline{D}_i g.$$

Now, due to some mathematical reasons we need to introduce the truncation operator  $R: \mathbb{R} \rightarrow \mathbb{R}$  given by

$$R(u) = u^+ - (u - \xi_m)^+, \tag{1}$$

where  $r^+ = \max\{0, r\}$  denotes the positive part of  $r$ . Moreover,  $\xi_m$  is a positive constant that we describe later.

Here, we are interested in the numerical analysis of the following problem which models the evolution of concentration of surfactant (see [1]):

$$c' - D \Delta c + \mathbf{u} \cdot \nabla c = 0 \quad \text{in } \Omega \times (0, T), \tag{2}$$

$$c = c_b \quad \text{on } \Gamma_D \times (0, T), \tag{3}$$

$$D \frac{\partial c}{\partial \boldsymbol{\nu}} = 0 \quad \text{on } \Gamma_N \times (0, T), \tag{4}$$

$$D \frac{\partial c}{\partial \boldsymbol{\nu}} = -S_\Gamma \quad \text{on } \Gamma_S \times (0, T), \tag{5}$$

$$c(\mathbf{x}, 0) = c_0(\mathbf{x}) \quad \text{for a.e. } \mathbf{x} \in \Omega, \tag{6}$$

$$\xi' - D_S \Delta_S \xi + \mathbf{u}_\tau \cdot \nabla_S \xi + \xi(\nabla_S \cdot \mathbf{u}) = S_\Gamma \text{ on } \Gamma_S \times (0, T), \tag{7}$$

$$D_S \nabla_S \xi \cdot \boldsymbol{\mu} = 0 \text{ on } \partial \Gamma_S \times (0, T), \tag{8}$$

$$\xi(\mathbf{x}, 0) = \xi_0(\mathbf{x}) \text{ for a.e. } \mathbf{x} \in \Gamma_S, \tag{9}$$

with the source term in (5) and (7) following the Langmuir–Hinshelwood kinetics and given by (see [1])

$$S_\Gamma(\mathbf{x}, t) = k_L^a c(\mathbf{x}, t) \left( 1 - \frac{R(\xi(\mathbf{x}, t))}{\xi_m} \right) - k_L^d \xi(\mathbf{x}, t). \tag{10}$$

In the previous coupled system of equations, the unknowns, represented by  $c(\mathbf{x}, t)$  and  $\xi(\mathbf{x}, t)$ , stand for the volumetric and surface surfactant concentrations, respectively, at point  $\mathbf{x}$  and time  $t \in (0, T)$ ,  $T > 0$  being the final time. Besides, a prime over a variable represents the time derivative,  $c_b$  denotes the bulk concentration, the positive constants  $D$  and  $D_S$  are the bulk and the surface diffusion coefficients, respectively,  $c_0$  is a function defined in  $\Omega$ , which gives the initial concentration of surfactant, and  $\xi_0$  is a function defined on  $\Gamma_S$  which denotes the initial surface concentration. Note that Eq. (7) allows diffusion along the surface  $\Gamma_S$ , and Eq. (10) describes the adsorption-desorption transport of surfactant molecules between the bulk phase and the surface, as stated in [1, 2]. The convective terms in (2) and (7) have been included here for the sake of completeness, where  $\mathbf{u}$  represents the velocity of the bulk molecules and  $\mathbf{u}_\tau$  its tangential component given by  $\mathbf{u}_\tau = \mathbf{u} - (\mathbf{u} \cdot \boldsymbol{\nu})\boldsymbol{\nu}$ . The positive constants  $k_L^a$  and  $k_L^d$  denote the adsorption and desorption rate constants, respectively, and  $\xi_m > 0$  is the maximum surface coverage.

*Remark 1* We note that in Eq. (10) we used the truncation function  $R$  only for mathematical reasons, in order to assure that function  $S_\Gamma$  is Lipschitz with respect to variables  $c$  and  $\xi$ . In [11] we also analyzed the problems with and without this truncation, giving some relations between their respective solutions.

We turn now to the weak formulation of problem (2)–(9). Let us consider the space

$$V = \left\{ v \in H^1(\Omega); v|_{\Gamma_D} = 0 \right\},$$

endowed with the inner product and the associated norm given by

$$((u, v)) = \int_\Omega \nabla u \cdot \nabla v \, dx, \quad \|v\|_V = ((v, v))^{1/2}.$$

We denote by  $V'$  the dual space to  $V$  and by  $\langle \cdot, \cdot \rangle$  the scalar product for the duality  $V', V$ . Moreover, we recall the inner product in  $H = L^2(\Omega)$  given by

$$(u, v)_H = \int_\Omega uv \, dx,$$

with the associated norm  $\|v\|_H = (v, v)_H^{1/2}$ . Furthermore, we consider the Hilbert space

$$\mathcal{W}(0, T) = \{v \in L^2(0, T; V); v' \in L^2(0, T; V')\},$$

the time derivative being understood in the distributional sense and endowed with the norm

$$\|v\|_{\mathcal{W}(0, T)}^2 = \|v\|_{L^2(0, T; V)}^2 + \|v'\|_{L^2(0, T; V')}^2.$$

It is well known (cf. e.g. [20]) that  $\mathcal{W}(0, T) \subset L^2(0, T; V) \subset L^2(0, T; H) \subset L^2(0, T; V')$  and  $\mathcal{W}(0, T) \subset \mathcal{C}([0, T]; H)$ , where all the embeddings are continuous. Here,  $\mathcal{C}([0, T]; H)$  stands for the space of continuous functions from  $[0, T]$  to  $H$ .

On the other hand, on the boundary  $\Gamma_S$  we consider the space  $X = L^2(\Gamma_S)$  with the inner product and norm given by

$$(u, v)_X = \int_{\Gamma_S} uv \, d\sigma, \quad \|v\|_X = (v, v)_X^{1/2},$$

$d\sigma$  being the surface element on  $\Gamma_S$  (see [14], page 389). Regarding Sobolev spaces on surfaces we also consider the space

$$H^1(\Gamma_S) = \{f \in X; \underline{D}_i f \in X, i = 1, \dots, d + 1\},$$

endowed with the inner product and its associated norm given by (see [9])

$$(u, v)_{H^1(\Gamma_S)} = \int_{\Gamma_S} uv \, d\sigma + \int_{\Gamma_S} \nabla_S u \cdot \nabla_S v \, d\sigma, \quad \|v\|_{H^1(\Gamma_S)} = (v, v)_{H^1(\Gamma_S)}^{1/2}.$$

Let  $\gamma: V \rightarrow X$  denote the trace operator on  $\Gamma_S$ . From the continuity of the trace operator (cf Theorem 3.9.34 in [8]), it follows that

$$\|\gamma v\|_X \leq K \|v\|_V \quad \text{for all } v \in V \text{ with } K = \|\gamma\|_{\mathcal{L}(V, X)}. \quad (11)$$

We denote by  $H^1(\Gamma_S)'$  the dual space to  $H^1(\Gamma_S)$ . Since  $\Gamma_S$  is a compact  $d$ -dimensional  $\mathcal{C}^{0,1}$ -manifold we consider the Gelfand triple (see [21, p. 267]):

$$H^1(\Gamma_S) \hookrightarrow X \hookrightarrow H^1(\Gamma_S)', \quad (12)$$

and we define the Banach space

$$\mathcal{W}_S(0, T) = \{v \in L^2(0, T; H^1(\Gamma_S)); v' \in L^2(0, T; H^1(\Gamma_S)')\}.$$

Thus, the space  $\mathcal{W}_S(0, T)$  is contained in  $\mathcal{C}([0, T]; X)$  (see [20], page 106).

We note that truncation operator  $R$  has the following properties which will be useful in the next section:

$$R \text{ is 1-Lipschitz continuous,}$$

$$0 \leq R(\eta(x)) \leq \xi_m \quad \text{for all } \eta \in X \text{ and a.e. } x \in \Gamma_S.$$

Finally, for the sake of simplicity in the writing, we assume that  $c_b = 0$  in the rest of the paper. It is straightforward to extend the analysis presented in the next section to more general situations.

Using Green’s formula, boundary conditions (3), (4), (5) and (8), and Eq. (10), we obtain the following weak formulation of problem (2)–(9).

**Problem P** Find  $c \in \mathcal{W}(0, T)$  and  $\xi \in \mathcal{W}_S(0, T)$  such that  $c(0) = c_0, \xi(0) = \xi_0$  and, for a.e.  $t \in (0, T)$ ,

$$\langle c'(t), v \rangle_{V' \times V} + D((c(t), v)) + k_L^a \left( \gamma c \left( 1 - \frac{R(\xi(t))}{\xi_m} \right), \gamma v \right)_X$$

$$+ (\mathbf{u}(t) \cdot \nabla c(t), v)_H = k_L^d(\xi(t), \gamma v)_X \quad \forall v \in V, \tag{13}$$

$$\langle \xi'(t), w \rangle_{H^1(\Gamma_S)' \times H^1(\Gamma_S)} + D_S \int_{\Gamma_S} \nabla_S \xi(t) \cdot \nabla_S w \, d\sigma + k_L^d(\xi(t), w)_X$$

$$= k_L^a \left( \gamma c(t) \left( 1 - \frac{R(\xi(t))}{\xi_m} \right), w \right)_X$$

$$- (\mathbf{u}_\tau(t) \cdot \nabla_S \xi(t) + \xi(t) \nabla_S \cdot \mathbf{u}(t), w)_X \quad \forall w \in H^1(\Gamma_S), \tag{14}$$

where we remark that we suppressed the dependence on the spatial variable for the sake of clarity.

We note that the initial conditions in Problem P make sense since  $\mathcal{W}(0, T) \subset \mathcal{C}([0, T]; H)$  and  $\mathcal{W}_S(0, T) \subset \mathcal{C}([0, T]; X)$ .

The following is the main result concerning Problem P (see [11] for details).

**Theorem 1** Assume that  $D, D_S, k_L^d, k_L^a$  and  $\xi_m$  are positive constants,  $c_0 \in H, \xi_0 \in X$  and  $\mathbf{u} \in L^\infty(0, T; L^\infty(\Omega; \mathbb{R}^{d+1}))$  with  $\nabla_S \cdot \mathbf{u} \in L^\infty(0, T; L^\infty(\Gamma_S))$  and  $\mathbf{u}_\tau \in L^\infty(0, T; L^\infty(\Gamma_S; \mathbb{R}^{d+1}))$ . Then Problem P has a unique solution  $c \in \mathcal{W}(0, T)$  and  $\xi \in \mathcal{W}_S(0, T)$ .

The proof of Theorem 1 is carried out in [11] and it is based on the study of two intermediate problems, followed by the application of the Schauder fixed-point theorem and Gronwall’s inequality.

### 3 Fully discrete approximation: a priori error estimates

In this section, we now introduce a finite element algorithm to approximate solutions to Problem P and we detail an a priori error analysis.

The discretization of Problem P is done as follows. First, we assume that  $\overline{\Omega}$  is a polyhedral domain and, to approximate the variational space  $V$ , we consider a finite dimensional space  $V^h \subset V$  given by

$$V^h = \left\{ v^h \in C(\overline{\Omega}); v^h|_K \in P_1(K) \quad \forall K \in \mathcal{T}^h, v^h = 0 \text{ on } \Gamma_D \right\}, \tag{15}$$

where  $P_1(K)$  represents the space of polynomials of global degree less or equal to one in  $K$  and we denote by  $(\mathcal{T}^h)_{h>0}$  a regular family of triangulations of  $\overline{\Omega}$  (in the sense of [7]), compatible with the partition of the boundary  $\partial\Omega$  into  $\Gamma_D, \Gamma_N$  and  $\Gamma_S$ ; i.e. the finite element space  $V^h$  is composed of continuous and piecewise affine functions. Let  $h_K$  be the diameter of an element  $K \in \mathcal{T}^h$  and let  $h = \max_{K \in \mathcal{T}^h} h_K$  denote the spatial discretization parameter. Moreover, let  $(\tilde{\mathcal{T}}^h)_{h>0}$  be the triangulation induced by  $(\mathcal{T}^h)_{h>0}$  onto  $\Gamma_S$ . Then, we construct the finite element space  $X^h$ , approximating the Sobolev space  $H^1(\Gamma_S)$ , in the form:

$$X^h = \left\{ w^h \in C(\overline{\Gamma_S}); w^h|_{\tilde{K}} \in P_1(\tilde{K}) \quad \forall \tilde{K} \in \tilde{\mathcal{T}}^h \right\}, \tag{16}$$

where  $P_1(\tilde{K})$  represents the space of polynomials of global degree less or equal to one in  $\tilde{K}$ .

Finally, we assume that the discrete initial conditions, denoted by  $c_0^h$  and  $\xi_0^h$ , are given by

$$c_0^h = \mathcal{P}_{V^h} c_0, \quad \xi_0^h = \mathcal{P}_{X^h} \xi_0, \tag{17}$$

where  $\mathcal{P}_{V^h}$  and  $\mathcal{P}_{X^h}$  are the classical finite element interpolation operators over the finite element spaces  $V^h$  and  $X^h$ , respectively (see, for instance, [7]).

To discretize the time derivatives, we consider a uniform partition of the time interval  $[0, T]$ , denoted by  $0 = t_0 < t_1 < \dots < t_N = T$ , and let  $k$  be the time step size,  $k = T/N$ . For a continuous function  $f(t)$ , let  $f_n = f(t_n)$  and, for a sequence  $\{w_n\}_{n=0}^N$ , we let  $\delta w_n = (w_n - w_{n-1})/k$  be its corresponding divided differences.

Finally, in order to simplify the writing, we assume, without loss of generality, that constants  $D, D_S, k_L^a, k_L^d, \xi_m$  are equal to 1 and we recall that  $c_b$  was assumed to be 0.

Therefore, using a combination of the implicit and explicit Euler schemes, we obtain the following fully discrete approximation of Problem P.

**Problem P<sup>h</sup>** Find  $c^{hk} = \{c_n^{hk}\}_{n=0}^N \subset V^h$  and  $\xi^{hk} = \{\xi_n^{hk}\}_{n=0}^N \subset X^h$  such that  $c_0^{hk} = c_0^h, \xi_0^{hk} = \xi_0^h$  and, for  $n = 1, \dots, N$ ,

$$\begin{aligned} & \left( \delta c_n^{hk}, v^h \right)_H + \left( c_n^{hk}, v^h \right) + \left( \mathbf{u}_n \cdot \nabla c_n^{hk}, v^h \right)_H + \left( \gamma c_n^{hk} \left( 1 - R \left( \xi_{n-1}^{hk} \right) \right), \gamma v^h \right)_X \\ & = \left( \xi_{n-1}^{hk}, \gamma v^h \right)_X, \quad \forall v^h \in V^h, \end{aligned} \tag{18}$$

$$\begin{aligned} & \left( \delta \xi_n^{hk}, w^h \right)_X + \int_{\Gamma_S} \nabla_S \xi_n^{hk} \cdot \nabla_S w^h \, d\sigma + \left( \xi_n^{hk}, w^h \right)_X = \left( \gamma c_n^{hk} \left( 1 - R \left( \xi_{n-1}^{hk} \right) \right), w^h \right)_X \\ & - \left( \mathbf{u}_\tau \cdot \nabla_S \xi_n^{hk} + \xi_n^{hk} \nabla_S \cdot \mathbf{u}_n, w^h \right)_X, \quad \forall w^h \in X^h. \end{aligned} \tag{19}$$

We note that it is straightforward to prove the coerciveness of the bilinear forms to obtain the existence of a unique solution to Problem  $P^h$ . Thus, we have the following.

**Theorem 2** *Let the assumptions of Theorem 1 hold. Then Problem  $P^h$  has a solution  $(c^{hk}, \xi^{hk}) \subset V^h \times X^h$ .*

In this section, assuming that  $\Gamma_S$  is  $C^\infty$  (i.e. a straight line if  $d = 1$  or a planar section if  $d = 2$ ), our aim is to obtain a priori error estimates on the numerical errors  $c_n - c_n^{hk}$  and  $\xi_n - \xi_n^{hk}$ . Then, we assume the following additional regularity on the continuous solution:

$$\begin{aligned} c & \in C^1([0, T]; H) \cap C([0, T]; V \cap L^\infty(\overline{\Gamma_S})), \\ \xi & \in C^1([0, T]; X) \cap C([0, T]; H^1(\Gamma_S)). \end{aligned} \tag{20}$$

Keeping in mind the additional regularity (20), we write variational equation (13), at time  $t = t_n$  and for  $v = v^h \in V^h \subset V$ , to obtain

$$\begin{aligned} & \left( c'_n, v^h \right)_H + \left( (c_n, v^h) \right) + \left( \mathbf{u}_n \cdot \nabla c_n, v^h \right)_H + \left( \gamma c_n (1 - R(\xi_n)), \gamma v^h \right)_X \\ & = \left( \xi_n, \gamma v^h \right)_X. \end{aligned} \tag{21}$$

Therefore, subtracting Eqs. (21) and (18) it follows that, for all  $v^h \in V^h$ ,

$$\begin{aligned} & \left( c'_n - \delta c_n^{hk}, v^h \right)_H + \left( (c_n - c_n^{hk}, v^h) \right) + \left( \mathbf{u}_n \cdot \nabla (c_n - c_n^{hk}), v^h \right)_H \\ & + \left( \gamma c_n (1 - R(\xi_n)) - \gamma c_n^{hk} (1 - R(\xi_{n-1}^{hk})), \gamma v^h \right)_X = \left( \xi_n - \xi_{n-1}^{hk}, \gamma v^h \right)_X, \end{aligned}$$

and so,

$$\begin{aligned} & \left( c'_n - \delta c_n^{hk}, c_n - c_n^{hk} \right)_H + \left( (c_n - c_n^{hk}, c_n - c_n^{hk}) \right) \\ & + \left( \mathbf{u}_n \cdot \nabla (c_n - c_n^{hk}), c_n - c_n^{hk} \right)_H \\ & + \left( \gamma c_n (1 - R(\xi_n)) - \gamma c_n^{hk} (1 - R(\xi_{n-1}^{hk})), \gamma (c_n - c_n^{hk}) \right)_X \\ & - \left( \xi_n - \xi_{n-1}^{hk}, \gamma (c_n - c_n^{hk}) \right)_X \\ & = \left( c'_n - \delta c_n^{hk}, c_n - v^h \right)_H \\ & + \left( (c_n - c_n^{hk}, c_n - v^h) \right) + \left( \mathbf{u}_n \cdot \nabla (c_n - c_n^{hk}), c_n - v^h \right)_H \end{aligned}$$



$$\begin{aligned}
 & + \left( \gamma c_n (1 - R(\xi_n)) - \gamma c_n^{hk} \left( 1 - R(\xi_{n-1}^{hk}) \right), \gamma (c_n - v^h) \right)_X \\
 & - \left( \xi_n - \xi_{n-1}^{hk}, \gamma (c_n - v^h) \right)_X.
 \end{aligned}$$

Now, keeping in mind the following estimates and properties

$$\begin{aligned}
 & (c'_n - \delta c_n^{hk}, v)_H = (c'_n - \delta c_n, v)_H + (\delta c_n - \delta c_n^{hk}, v)_H, \\
 & |(c'_n - \delta c_n, v)_H| \leq C \|c'_n - \delta c_n\|_H^2 + \epsilon \|v\|_H^2, \\
 & (\delta c_n - \delta c_n^{hk}, c_n - c_n^{hk})_H \geq \frac{1}{2k} \left( \|c_n - c_n^{hk}\|_H^2 - \|c_{n-1} - c_{n-1}^{hk}\|_H^2 \right), \\
 & |(u_n \cdot \nabla (c_n - c_n^{hk}), v)| \leq \epsilon \|c_n - c_n^{hk}\|_V^2 + C \|v\|_H^2, \\
 & \left| \left( \gamma c_n (1 - R(\xi_n)) - \gamma c_n^{hk} \left( 1 - R(\xi_{n-1}^{hk}) \right), \gamma v \right)_X \right| \\
 & = \left| \left( (\gamma c_n - \gamma c_n^{hk}) \left( 1 - R(\xi_{n-1}^{hk}) \right) - \gamma c_n \left( R(\xi_n) - R(\xi_{n-1}^{hk}) \right), \gamma v \right)_X \right| \\
 & \leq C \left( \left\| \gamma (c_n - c_n^{hk}) \right\|_X^2 + \left\| \xi_n - \xi_{n-1}^{hk} \right\|_X^2 + \|v\|_X^2 \right), \\
 & \left( (1 - R(\xi_{n-1}^{hk})) \gamma (c_n - c_n^{hk}), \gamma (c_n - c_n^{hk}) \right)_X \geq 0, \\
 & (\xi_n - \xi_{n-1}^{hk}, \gamma v)_X \leq C \left( \left\| \xi_n - \xi_{n-1}^{hk} \right\|_X^2 + \|\gamma v\|_X^2 \right), \\
 & \|\gamma v\|_X^2 \leq \|v\|_V^2,
 \end{aligned}$$

where  $\epsilon$  is a positive parameter assumed to be small,  $C$ , here and in what follows, is a positive constant which is independent of the discretization parameters  $h$  and  $k$ , but possibly depending on the continuous solution  $c$  and  $\xi$ , and we denote  $\delta c_n = (c_n - c_{n-1})/k$ . After easy algebra we obtain the following

$$\begin{aligned}
 & \|c_n - c_n^{hk}\|_H^2 + Ck \|c_n - c_n^{hk}\|_V^2 \leq Ck \left( \|c_n - v^h\|_V^2 + \left\| \xi_n - \xi_{n-1}^{hk} \right\|_X^2 \right. \\
 & \quad \left. + \|c'_n - \delta c_n\|_H^2 + \|c_n - c_n^{hk}\|_H^2 + (\delta c_n - \delta c_n^{hk}, c_n - v^h)_H \right) \\
 & \quad + \|c_{n-1} - c_{n-1}^{hk}\|_H^2, \quad \forall v^h \in V^h.
 \end{aligned}$$

Therefore, by induction we find that, for all  $\{v_j^h\}_{j=1}^n \subset V^h$ ,

$$\begin{aligned}
 & \|c_n - c_n^{hk}\|_H^2 + Ck \sum_{j=1}^n \|c_j - c_j^{hk}\|_V^2 \leq Ck \sum_{j=1}^n \left( \|c_j - v_j^h\|_V^2 + \left\| \xi_j - \xi_j^{hk} \right\|_X^2 + k^2 \right. \\
 & \quad \left. + \|c'_j - \delta c_j\|_H^2 + \|c_j - c_j^{hk}\|_H^2 + (\delta c_j - \delta c_j^{hk}, c_j - v_j^h)_H \right) + \|c_0 - c_0^h\|_H^2.
 \end{aligned} \tag{22}$$

Now, keeping in mind again the additional regularity (20), we write variational equation (14), at time  $t = t_n$  and for  $w = w^h \in X^h \subset H^1(\Gamma_S)$ , to obtain

$$\begin{aligned} & \left(\xi'_n, w^h\right)_X + \int_{\Gamma_S} \nabla_S \xi_n \cdot \nabla_S w^h \, d\sigma + \left(\xi_n, w^h\right)_X = \left(\gamma c_n (1 - R(\xi_n)), w^h\right)_X \\ & - \left((\mathbf{u}_\tau)_n \cdot \nabla_S \xi_n + (\nabla_S \cdot \mathbf{u}_n) \xi_n, w^h\right)_X, \quad \forall w^h \in X^h. \end{aligned} \tag{23}$$

Subtracting variational equations (23) and (19) we have

$$\begin{aligned} & \left(\xi'_n - \delta \xi_n^{hk}, w^h\right)_X + \int_{\Gamma_S} \nabla_S (\xi_n - \xi_n^{hk}) \cdot \nabla_S w^h \, d\sigma + \left(\xi_n - \xi_n^{hk}, w^h\right)_X \\ & = \left(\gamma c_n (1 - R(\xi_n)) - \gamma c_n^{hk} (1 - R(\xi_{n-1}^{hk})), w^h\right)_X \\ & - \left((\mathbf{u}_\tau)_n \cdot \nabla_S (\xi_n - \xi_n^{hk}) + (\xi_n - \xi_n^{hk}) \nabla_S \cdot \mathbf{u}_n, w^h\right)_X, \quad \forall w^h \in X^h, \end{aligned}$$

and thus,

$$\begin{aligned} & \left(\xi'_n - \delta \xi_n^{hk}, \xi_n - \xi_n^{hk}\right)_X + \int_{\Gamma_S} \nabla_S (\xi_n - \xi_n^{hk}) \cdot \nabla_S (\xi_n - \xi_n^{hk}) \, d\sigma \\ & + \left(\xi_n - \xi_n^{hk}, \xi_n - \xi_n^{hk}\right)_X - \left(\gamma c_n (1 - R(\xi_n)) - \gamma c_n^{hk} (1 - R(\xi_{n-1}^{hk})), \xi_n - \xi_n^{hk}\right)_X \\ & + \left((\mathbf{u}_\tau)_n \nabla_S (\xi_n - \xi_n^{hk}) + (\xi_n - \xi_n^{hk}) \nabla_S \cdot \mathbf{u}_n, \xi_n - \xi_n^{hk}\right)_X \\ & = \left(\xi'_n - \delta \xi_n^{hk}, \xi_n - w^h\right)_X + \int_{\Gamma_S} \nabla_S (\xi_n - \xi_n^{hk}) \cdot \nabla_S (\xi_n - w^h) \, d\sigma \\ & + \left(\xi_n - \xi_n^{hk}, \xi_n - w^h\right)_X - \left(\gamma c_n (1 - R(\xi_n)) - \gamma c_n^{hk} (1 - R(\xi_{n-1}^{hk})), \xi_n - w^h\right)_X \\ & + \left((\mathbf{u}_\tau)_n \nabla_S (\xi_n - \xi_n^{hk}) + (\xi_n - \xi_n^{hk}) \nabla_S \cdot \mathbf{u}_n, \xi_n - w^h\right)_X, \quad \forall w^h \in X^h. \end{aligned}$$

Now, taking into account the following estimates and properties

$$\begin{aligned} & \left(\xi'_n - \delta \xi_n^{hk}, w\right)_X = \left(\xi'_n - \delta \xi_n, w\right)_X + \left(\delta \xi_n - \delta \xi_n^{hk}, w\right)_X, \\ & \left|\left(\xi'_n - \delta \xi_n, w\right)_X\right| \leq C \left\|\xi'_n - \delta \xi_n\right\|_X^2 + \epsilon \|w\|_X^2, \\ & \left(\delta \xi_n - \delta \xi_n^{hk}, \xi_n - \xi_n^{hk}\right)_X \geq \frac{1}{2k} \left(\left\|\xi_n - \xi_n^{hk}\right\|_X^2 - \left\|\xi_{n-1} - \xi_{n-1}^{hk}\right\|_X^2\right), \\ & \left|(\nabla_S \cdot \mathbf{u}_n) (\xi_n - \xi_n^{hk}), w\right)_X \right| \leq C \left(\left\|\xi_n - \xi_n^{hk}\right\|_X^2 + \|w\|_X^2\right), \\ & \left|\left(\gamma c_n (1 - R(\xi_n)) - \gamma c_n^{hk} (1 - R(\xi_{n-1}^{hk})), w\right)_X\right| \\ & = \left|\left(\left(\gamma c_n - \gamma c_n^{hk}\right) (1 - R(\xi_{n-1}^{hk})) - \gamma c_n (R(\xi_n) - R(\xi_{n-1}^{hk})), w\right)_X\right| \\ & \leq C \left(\left\|\gamma (c_n - c_n^{hk})\right\|_X^2 + \left\|\xi_n - \xi_{n-1}^{hk}\right\|_X^2 + \|w\|_X^2\right), \end{aligned}$$

$$\begin{aligned} (\xi_n - \xi_n^{hk}, w)_X &\leq C \left( \|\xi_n - \xi_n^{hk}\|_X^2 + \|w\|_X^2 \right), \\ \left| \left( (u_\tau)_n \cdot \nabla_S (\xi_n - \xi_n^{hk}), w \right)_X \right| &\leq \epsilon \left\| \nabla_S (\xi_n - \xi_n^{hk}) \right\|_{[L^2(\Gamma_S)]^d}^2 + C \|w\|_X^2, \end{aligned}$$

where  $\epsilon$  is again a positive parameter assumed to be small and we denote  $\delta\xi_n = (\xi_n - \xi_{n-1})/k$ , after easy algebra it follows that

$$\begin{aligned} \|\xi_n - \xi_n^{hk}\|_X^2 + Ck \|\nabla_S (\xi_n - \xi_n^{hk})\|_{[L^2(\Gamma_S)]^d}^2 &\leq Ck \left( \|\xi_n - w^h\|_{H^1(\Gamma_S)}^2 + \|\xi_n - \xi_n^{hk}\|_X^2 \right. \\ &+ \|\xi_n - \xi_{n-1}^{hk}\|_X^2 + \|\xi'_n - \delta\xi_n\|_X^2 + \|c_n - c_n^{hk}\|_V^2 + \left. \left( \delta\xi_n - \delta\xi_n^{hk}, \xi_n - w^h \right)_X \right) \\ &+ \|\xi_{n-1} - \xi_{n-1}^{hk}\|_X^2, \quad \forall w^h \in X^h. \end{aligned}$$

Thus, again by induction we obtain the following estimates for the surface concentration,

$$\begin{aligned} \|\xi_n - \xi_n^{hk}\|_X^2 + Ck \sum_{j=1}^n \|\nabla_S (\xi_j - \xi_j^{hk})\|_{[L^2(\Gamma_S)]^d}^2 &\leq Ck \sum_{j=1}^n \left( \|\xi_j - w_j^h\|_{H^1(\Gamma_S)}^2 + k^2 \right. \\ &+ \|\xi_j - \xi_j^{hk}\|_X^2 + \|\xi'_j - \delta\xi_j\|_X^2 + \|c_j - c_j^{hk}\|_V^2 + \left. \left( \delta\xi_j - \delta\xi_j^{hk}, \xi_j - w_j^h \right)_X \right) \\ &+ \|\xi_0 - \xi_0^h\|_X^2, \quad \forall \{w_j^h\}_{j=1}^n \subset X^h. \end{aligned} \tag{24}$$

Combining now estimates (22) and (24) we have, for all  $\{v_j^h\}_{j=1}^n \subset V^h$  and  $\{w_j^h\}_{j=1}^n \subset X^h$ ,

$$\begin{aligned} \|c_n - c_n^{hk}\|_H^2 + \|\xi_n - \xi_n^{hk}\|_X^2 + Ck \sum_{j=1}^n \left[ \|c_j - c_j^{hk}\|_V^2 + \|\nabla_S (\xi_j - \xi_j^{hk})\|_{[L^2(\Gamma_S)]^d}^2 \right] \\ \leq Ck \sum_{j=1}^n \left( \|c_j - v_j^h\|_V^2 + \|\xi_j - \xi_j^{hk}\|_X^2 + \|c'_j - \delta c_j\|_H^2 + \|c_j - c_j^{hk}\|_H^2 + k^2 \right. \\ \left. + \left( \delta c_j - \delta c_j^{hk}, c_j - v_j^h \right)_H + \|\xi_j - w_j^h\|_{H^1(\Gamma_S)}^2 + \|\xi_j - \xi_j^{hk}\|_X^2 + \|\xi'_j - \delta\xi_j\|_X^2 \right. \\ \left. + \left( \delta\xi_j - \delta\xi_j^{hk}, \xi_j - w_j^h \right)_X \right) + \|c_0 - c_0^h\|_H^2 + \|\xi_0 - \xi_0^h\|_X^2. \end{aligned}$$

Finally, taking into account that

$$\begin{aligned} \sum_{j=1}^n k \left( \delta c_j - \delta c_j^{hk}, c_j - v_j^h \right)_H &= \left( c_n - c_n^{hk}, c_n - v_n^h \right)_H + \left( c_0^h - c_0, c_1 - v_1^h \right)_H \\ &+ \sum_{j=1}^{n-1} \left( c_j - c_j^{hk}, c_j - v_j^h - \left( c_{j+1} - v_{j+1}^h \right) \right)_H, \end{aligned}$$

$$\sum_{j=1}^n k \left( \delta \xi_j - \delta \xi_j^{hk}, \xi_j - w_j^h \right)_X = \left( \xi_n - \xi_n^{hk}, \xi_n - w_n^h \right)_X + \left( \xi_0^h - \xi_0, \xi_1 - w_1^h \right)_X + \sum_{j=1}^{n-1} \left( \xi_j - \xi_j^{hk}, \xi_j - w_j^h - \left( \xi_{j+1} - w_{j+1}^h \right) \right)_X,$$

applying a discrete version of Gronwall’s inequality (see, e.g., [5]), we obtain the following a priori error estimates result.

**Theorem 3** *Let the assumptions of Theorem 1 and the additional regularities (20) hold. If we denote by  $(c, \xi)$  and  $(c^{hk}, \xi^{hk})$  the respective solutions to problems  $P$  and  $P^h$ , respectively, then the following estimates are obtained, for all  $v^h = \{v_n^{hk}\}_{n=0}^N \subset V^h$  and  $w^h = \{w_n^{hk}\}_{n=0}^N \subset X^h$ ,*

$$\begin{aligned} & \max_{0 \leq n \leq N} \left[ \|c_n - c_n^{hk}\|_H^2 + \|\xi_n - \xi_n^{hk}\|_X^2 \right] \\ & + k \sum_{j=1}^N \left( \|c_j - c_j^{hk}\|_V^2 + \|\nabla_S (\xi_j - \xi_j^{hk})\|_{[L^2(\Gamma_S)]^d}^2 \right) \\ & \leq Ck \sum_{j=1}^N \left( \|c_j - v_j^h\|_V^2 + \|c'_j - \delta c_j\|_H^2 + \|\xi_j - w_j^h\|_{H^1(\Gamma_S)}^2 + \|\xi'_j - \delta \xi_j\|_X^2 \right) \\ & + Ck^2 + Ck^{-1} \sum_{j=1}^{N-1} \|c_j - v_j^h - (c_{j+1} - v_{j+1}^h)\|_H^2 + C \max_{0 \leq n \leq N} \|c_n - v_n^h\|_H^2 \\ & + Ck^{-1} \sum_{j=1}^{N-1} \|\xi_j - w_j^h - (\xi_{j+1} - w_{j+1}^h)\|_X^2 + C \max_{0 \leq n \leq N} \|\xi_n - w_n^h\|_X^2 \\ & + C \|c_0 - c_0^h\|_H^2 + C \|\xi_0 - \xi_0^h\|_X^2. \end{aligned} \tag{25}$$

Estimates (25) are the basis for the analysis of the convergence rate. Hence, as an example, assume the following additional regularity conditions on the continuous solution:

$$\begin{aligned} c & \in C([0, T]; H^2(\Omega)) \cap H^2(0, T; H) \cap H^1(0, T; V), \\ \xi & \in C([0, T]; H^2(\Gamma_S)) \cap H^2(0, T; X) \cap H^1(0, T; H^1(\Gamma_S)). \end{aligned} \tag{26}$$

From these regularities, taking into account the approximation properties of the finite element interpolation operators we easily obtain that (see [7])

$$\|c_0 - c_0^h\|_H^2 + \|\xi_0 - \xi_0^h\|_X^2 \leq Ch^2.$$

We have the following.

**Corollary 1** *Let the assumptions of Theorem 3 and the additional regularities (26) hold. Then, the numerical approximation of Problem P by Problem P<sup>h</sup> is linearly convergent; that is, there exists a positive constant C, independent of the discretization parameters h and k, such that*

$$\max_{0 \leq n \leq N} \left[ \|c_n - c_n^{hk}\|_H + \|\xi_n - \xi_n^{hk}\|_X \right] \leq C(h + k).$$

The proof of Corollary 1 is done by using the classical properties on the approximation by the finite element spaces and the finite element interpolation operators P<sub>V<sup>h</sup></sub> and P<sub>X<sup>h</sup></sub> (see again [7]), and taking into account that (see [3,5] for details),

$$\begin{aligned} & k^{-1} \sum_{j=1}^{N-1} \left( \|c_j - v_j^h - (c_{j+1} - v_{j+1}^h)\|_H^2 + \|\xi_j - w_j^h - (\xi_{j+1} - w_{j+1}^h)\|_X^2 \right) \\ & \leq Ch^2 \left( \|c\|_{H^1(0,T;V)}^2 + \|\xi\|_{H^1(0,T;H^1(\Gamma_S))}^2 \right), \\ & k \sum_{j=1}^N \left( \|c'_j - \delta c_j\|_H^2 + \|\xi'_j - \delta \xi_j\|_X^2 \right) \leq Ck^2 \left( \|c\|_{H^2(0,T;H)}^2 + \|\xi\|_{H^2(0,T;X)}^2 \right). \end{aligned}$$

### 4 Numerical results

In order to verify the behaviour of the numerical method described in the previous section, some numerical experiments have been performed both in two- and three-dimensional problems.

#### 4.1 Numerical scheme

Given the solution c<sup>hk</sup><sub>n-1</sub> and ξ<sup>hk</sup><sub>n-1</sub> at time t<sub>n-1</sub>, the discrete volumetric surfactant concentration c<sup>hk</sup><sub>n</sub> is obtained from the following discrete linear variational equation, for all v<sup>h</sup> ∈ V<sup>h</sup>,

$$\begin{aligned} & (c_n^{hk}, v^h)_H + kD((c_n^{hk}, v^h)) + k k_L^a \left( \gamma c_n^{hk} \left( 1 - \frac{R(\xi_{n-1}^{hk})}{\xi_m} \right), \gamma v^h \right)_X \\ & + k \left( \mathbf{u}_n \cdot \nabla c_n^{hk}, v^h \right) = (c_{n-1}^{hk}, v^h)_H + k k_L^d \left( \xi_{n-1}^{hk}, \gamma v^h \right)_X. \end{aligned}$$

Later, we get the discrete surface concentration ξ<sup>hk</sup><sub>n</sub> from the discrete linear variational equation, for all w<sup>h</sup> ∈ X<sup>h</sup>,

$$\left( \xi_n^{hk}, w^h \right)_X + kD_S \int_{\Gamma_S} \nabla_S \xi_n^{hk} \cdot \nabla_S w^h \, d\sigma + k \left( (\mathbf{u}_\tau)_n \cdot \nabla_S \xi_n^{hk} + \xi_n^{hk} \nabla_S \cdot \mathbf{u}_n, w^h \right)_X$$

$$+ k k_L^d (\xi_n^{hk}, w^h)_X = (\xi_{n-1}^{hk}, w^h)_X + k k_L^a \left( \gamma c_n^{hk} \left( 1 - \frac{R(\xi_{n-1}^{hk})}{\xi_m} \right), w^h \right)_X .$$

We note that both numerical problems lead to linear non-symmetric systems and so, the classical LU method was applied for their solution.

The numerical scheme was implemented using FreeFEM++ (see [15] for details) on a Intel Core i5-3337U @ 1.80 GHz and a typical 3d run (100 step times and 10,000 nodes) took about 22 s of CPU time.

### 4.2 A first example: numerical convergence on a 2d domain

Our aim here is to show the numerical convergence of the finite element scheme. Therefore, a sequence of uniform partitions of both the time interval and the domain  $\Omega = [0, 1] \times [0, 1]$  into  $2(nd)^2$  triangles, has been performed (the finite element mesh corresponding to  $nd = 8$  is plotted on the right-hand side of Fig. 1).  $\Gamma_S = [0, 1] \times \{1\}$  has been selected as the surface of diffusion, and so we have  $(nd + 1)^2$  and  $nd + 1$  degrees of freedom for the volumetric and surface surfactant concentration problems, respectively.

The solutions obtained with  $nd = 1024$  and  $k = 0.0005$  have been considered as the “exact solutions”, while the numerical errors are given by

$$E^{hk} = \max_{0 \leq n \leq N} \left( \|c_n - c_n^{hk}\|_H + \|\xi_n - \xi_n^{hk}\|_X \right) .$$

The physical setting of the example is depicted in Fig. 1 (left-hand side), and the following data have been employed in the simulations:

$$T = 1 \text{ s}, \quad c_b = 3, \quad D = 1, \quad D_S = 1, \quad k_L^a = 1, \quad k_L^d = 1, \quad \xi_m = 1, \\ \mathbf{u} = \mathbf{0}, \quad c_0(x, y) = 3(1 - y) \text{ and } \xi_0(x) = 0 \quad \text{for } x, y \in [0, 1].$$

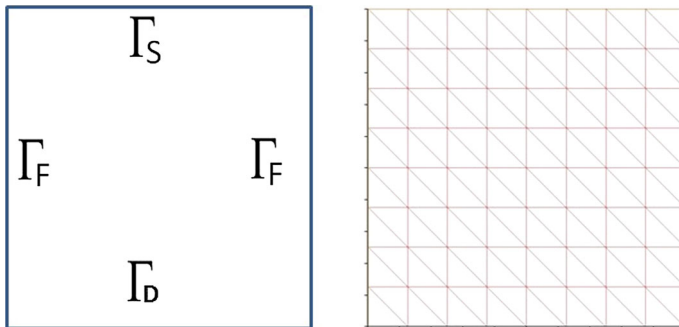
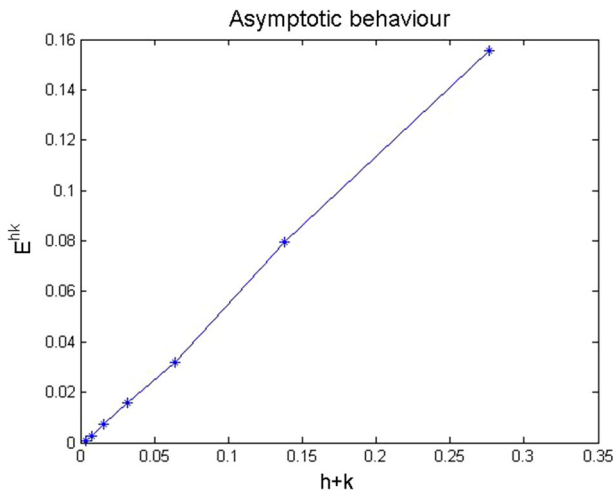


Fig. 1 Example 1: physical setting and mesh example for  $nd = 8$ .

**Table 1** Example 1: numerical errors ( $\times 10^2$ ) for some  $nd$  and  $k$ 

$nd$	$k$						
	0.001	0.002	0.005	0.01	0.02	0.05	0.1
8	0.009968	0.026507	0.076216	0.158685	0.321974	0.799018	1.554957
16	0.008719	0.025334	0.075073	0.157521	0.320742	0.797565	1.553153
32	0.008419	0.025043	0.074781	0.157220	0.320422	0.797190	1.552692
64	0.008345	0.024970	0.074707	0.157145	0.320341	0.797094	1.552575
128	0.008327	0.024952	0.074688	0.157125	0.320320	0.797070	1.552550
256	0.008323	0.024947	0.074683	0.157121	0.320315	0.797064	1.552536
512	0.008321	0.024946	0.074682	0.157119	0.320314	0.797063	1.552536

**Fig. 2** Example 1: asymptotic behaviour of the numerical scheme

In Table 1 the numerical errors obtained for some  $nd$  and  $k$  are shown. The evolution of the error versus the parameter  $k + h$  is plotted in Fig. 2 (here,  $h = \frac{\sqrt{2}}{nd}$ ). The linear convergence of the algorithm, stated in Corollary 1, seems to be achieved.

### 4.3 Second example: a 3d example

As a second test, the prism  $[0, 10^{-5}] \times [0, 10^{-5}] \times [0, 10^{-4}]$  is considered as the physical domain, with  $\Gamma_D$  as the lower boundary ( $\Gamma_D = [0, 10^{-5}] \times [0, 10^{-5}] \times \{0\}$ ) and  $\Gamma_S$  as the upper one ( $\Gamma_S = [0, 10^{-5}] \times [0, 10^{-5}] \times \{10^{-4}\}$ ).

Taking the value of the different parameters from [6], a solution of propanol is considered, and we employ the following data:

$$c_b = 333 \text{ mol/m}^3, \quad D = 5.2 \times 10^{-10} \text{ m}^2/\text{s}, \quad D_S = 5.2 \times 10^{-10} \text{ m}^2/\text{s}, \\ k_L^a = 7.8 \times 10^{-6} \text{ m/s}, \quad k_L^d = 199.74392 \text{ s}^{-1}, \quad \xi_m = 7.1 \times 10^{-6},$$

$$\mathbf{u}(\mathbf{x}) = 100(yz, xz, xy), \quad c_0(\mathbf{x}) = c_b(10^4 - z) \times 10^{-4} \text{ mol/m}^3 \quad \text{for all } \mathbf{x} = (x, y, z) \in \Omega, \\ \xi_0(\mathbf{x}) = 0 \text{ mol/m}^2 \quad \text{for all } \mathbf{x} \in \Gamma_S.$$

Using an structured mesh with 6561 nodes ( $h \approx 1.77 \times 10^{-6}$ ) and a time discretization parameter of  $k = 10^{-3}$ , we leave the solution evolve for  $T = 10 \text{ s}$ . In the left-hand side of Fig. 3 the isolines of the volumetric concentration of surfactant are depicted at final time, while in the right-hand side the evolution in time of the surface concentration at the center point is shown.

We note that with the data of the previous simulation, by using the initial condition of  $c_0(\mathbf{x}) = c_b$  for all  $\mathbf{x} \in \Omega$ , no velocity in the bulk ( $\mathbf{u} = \mathbf{0}$ ), and a value of  $k = 10^{-5} \text{ s}$  (for a total time of  $T = 0.1 \text{ s}$ ), the results of the simulation match with those obtained in [10] with a one-dimensional model, coinciding the experimental data from [16] for the superficial tension  $\gamma$ , which is given by

$$\gamma(t) = \gamma_0 - n R \theta \xi_m \log \left( \frac{\xi_m}{\xi_m - \xi(t)} \right),$$

where  $\gamma_0 = 0.0725 \text{ N/m}$  denotes the surface tension of pure water,  $\theta = 293 \text{ K}$  the temperature,  $R = 8.31 \text{ J/(K mol)}$  is the gas constant and  $n$  is a constant which is equal to one for a non-ionic surfactant. It can be observed in Fig. 4 the evolution in time, in the center of the upper surface, at point  $\mathbf{x} = (5 \times 10^{-6}, 5 \times 10^{-6}, 10^{-4})$ , of both the volumetric concentration and the superficial tension, the last one in logarithmic scale.

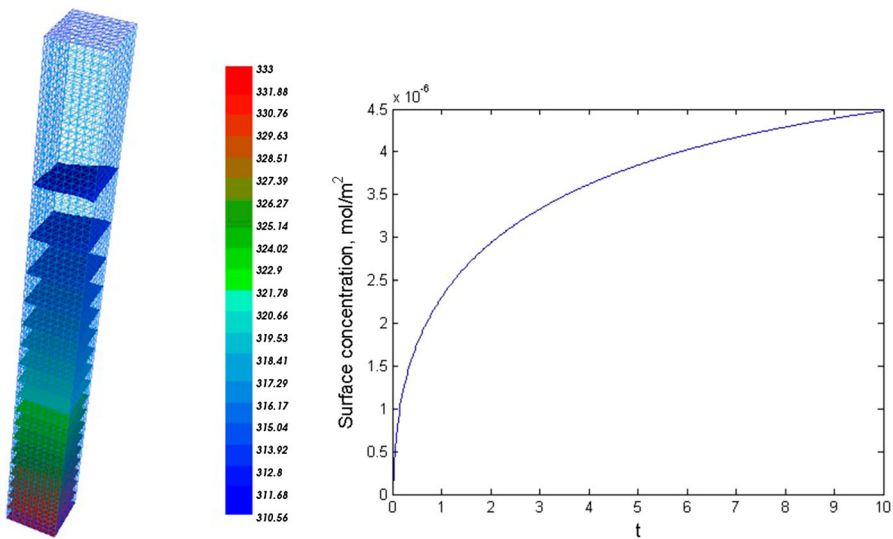


**Fig. 3** Example 2: final volumetric concentration ( $\text{mol/m}^3$ ) and evolution in time of the surface concentration ( $\text{mol/m}^2$ ) at the center point, respectively



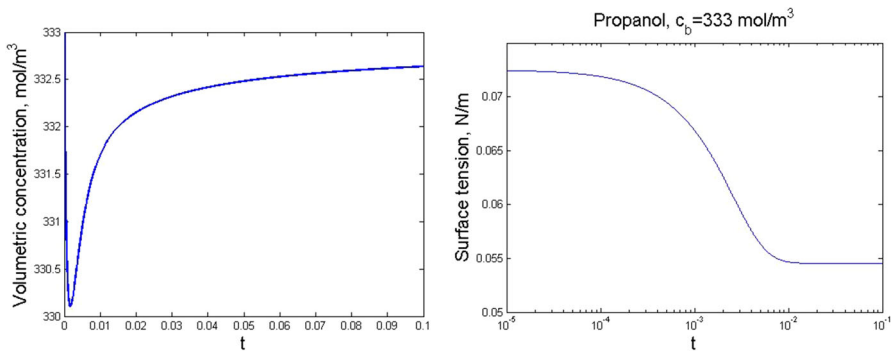


**Fig. 4** Example 2: evolution in time of the volumetric surfactant concentration and the superficial tension

#### 4.4 Third example: diffusion effect

As a final test, the domain  $\Omega = [0, 10^{-4}] \times [0, 10^{-4}] \times [0, 5 \times 10^{-5}]$  has been considered,  $\Gamma_S$  being the whole upper boundary ( $\Gamma_S = [0, 10^{-4}] \times [0, 10^{-4}] \times \{5 \times 10^{-5}\}$ ), and  $\Gamma_D$  the central region of the lower boundary ( $\Gamma_D = [2.5 \times 10^{-5}, 7.5 \times 10^{-5}] \times [2.5 \times 10^{-5}, 7.5 \times 10^{-5}] \times \{0\}$ ).

By using the same data for propanol employed in the previous example, now the conditions of this simulation correspond with the following data:

$$T = 0.5 \text{ s}, \quad c_b = 1 \text{ mol/m}^3, \quad \mathbf{u} = \mathbf{0}, \quad \xi_0 = 0 \text{ mol/m}^2.$$

Moreover, the initial condition for the volumetric concentration of surfactant is given as the value of  $c_b$  on the vertical part of the boundary  $\Gamma_D$ , vanishing in the rest of the domain, that is,

$$c_0(x, y, z) = \begin{cases} c_b & \text{if } (x, y) \in [2.5 \times 10^{-5}, 7.5 \times 10^{-5}] \times [2.5 \times 10^{-5}, 7.5 \times 10^{-5}], \\ 0 & \text{elsewhere.} \end{cases}$$

In Fig. 5 the evolution in time of the volumetric concentration at the upper central node ( $5 \times 10^{-5}, 5 \times 10^{-5}, 5 \times 10^{-5}$ ) is plotted. We can see an initial decay and recovery of the volumetric concentration, due to the equilibrium with the surface concentration, while after about 0.1 s, there is a maintained decay due to the diffusion of the surfactant.

In Fig. 6 (left-hand side) the evolution in time of the surface concentration at the same upper central node is plotted for different values of the surface diffusion coefficient  $D_S$  (related to the volumetric diffusion coefficient  $D$  and even a zero value). The evolution in time of the surface concentration shows an initial raising until the equilibrium with the surface concentration, and later another decay of the concentration, due to the equilibrium with a volumetric concentration which also decreases caused by the diffusion effect. We note that the results are rather similar for all these values of the coefficient and only if we apply a zoom at time  $t = 0.1$  s small differences can be observed (right-hand side). A possible explanation of this behaviour

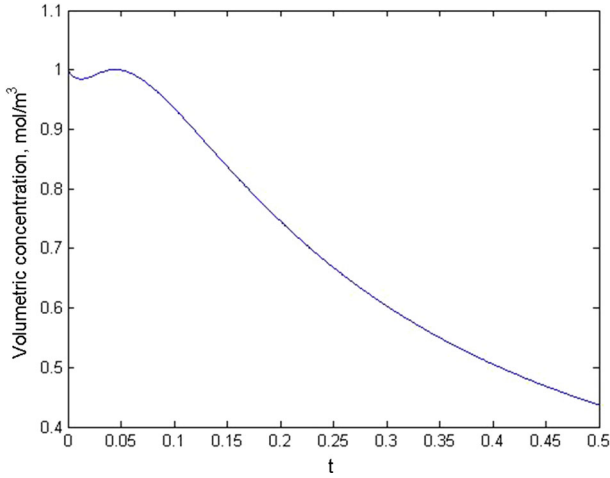


Fig. 5 Example 3: evolution in time of volumetric concentration at the middle point (mol/m<sup>3</sup>)

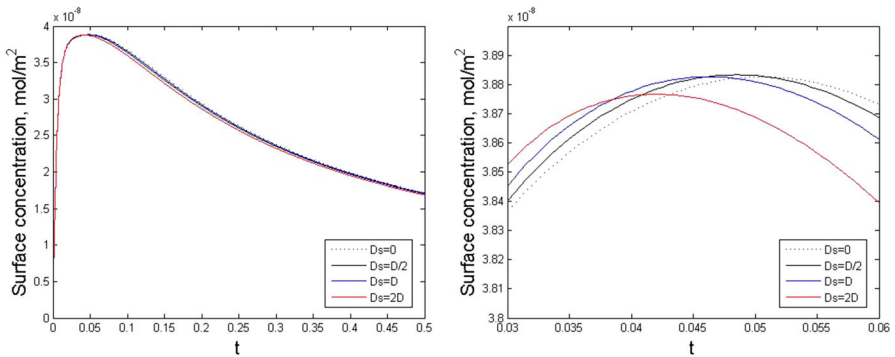


Fig. 6 Example 3: evolution in time of surface concentration (mol/m<sup>2</sup>) for different values of the surface diffusion coefficient (*left*) and zoom at time  $t = 0.1$  s (*right*)

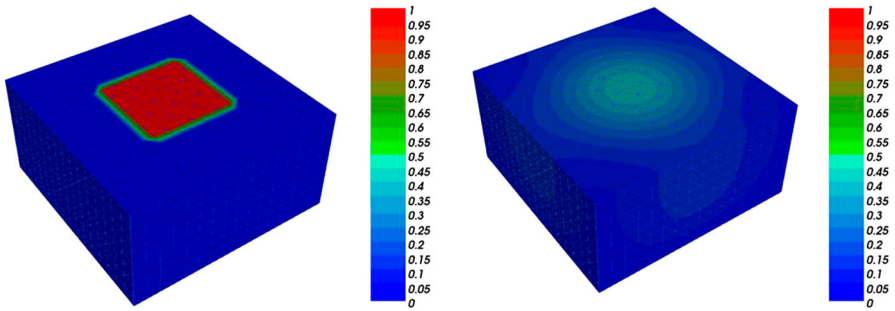
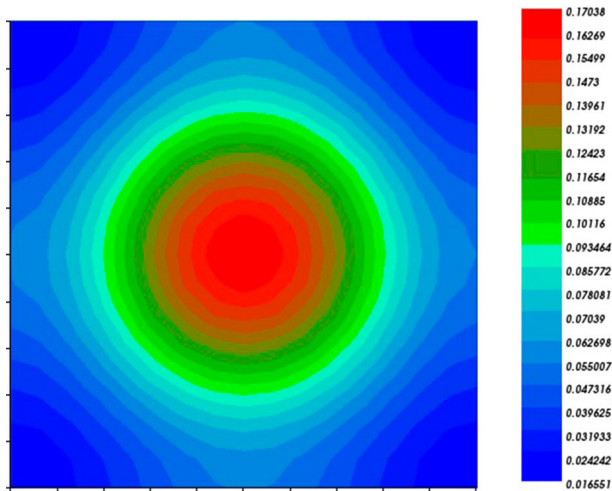


Fig. 7 Example 3: initial and final volumetric surfactant concentrations (mol/m<sup>3</sup>), respectively



**Fig. 8** Example 3: final surface surfactant concentration on  $\Gamma_S$  ( $\times 10^7$ ) ( $\text{mol}/\text{m}^2$ )

is that the surface concentration depends more on the volumetric concentration than on the surface diffusion.

Finally, in Fig. 7 both the initial conditions and the final volumetric concentrations are shown from a top view, while in Fig. 8 the diffusion of the surface concentration on  $\Gamma_S$  is presented. We can clearly observe the diffusion effect in both concentrations.

## 5 Conclusions

In this work we considered a new multidimensional mixed-kinetic adsorption model for the evolution of the surfactant concentrations. The model was written as a coupled system of nonlinear parabolic partial differential equations: a convective diffusion equation for the bulk surfactant concentration in the domain and a surface diffusion equation for its surface concentration on a manifold. The corresponding variational formulation was derived, for which a fully discrete approximation was introduced by using the finite element method and the implicit Euler scheme. A priori error estimates were proved, and the linear convergence of the algorithm was deduced under suitable additional regularity conditions. Finally, some numerical simulations were performed to show the accuracy of the approximation and the behaviour of the solutions.

We would like to remark that this work is a first step to use this model in more realistic situations. In particular, as a future work we plan to extend the algorithm we implemented here to the case of non-planar manifolds, as it occurs for instance in the bubbles.

## References

1. S. Adami, X.Y. Hu, N.A. Adams, A conservative SPH method for surfactant dynamics. *J. Comput. Phys.* **229**, 1909–1926 (2010)

2. S. Adami, X.Y. Hu, N.A. Adams, A new surface-tension formulation for multi-phase SPH using a reproducing divergence approximation. *J. Comput. Phys.* **229**, 5011–5021 (2010)
3. K.T. Andrews, J.R. Fernández, M. Shillor, Numerical analysis of dynamic thermoviscoelastic contact with damage of a rod. *IMA J. Appl. Math.* **70**(6), 768–795 (2005)
4. T. Aubin, *Nonlinear Analysis in Manifolds: Monge–Ampère Equations* (Springer, Berlin, 1982)
5. M. Campo, J.R. Fernández, K.L. Kuttler, M. Shillor, J.M. Viaño, Numerical analysis and simulations of a dynamic frictionless contact problem with damage. *Comput. Methods Appl. Mech. Eng.* **196**(1–3), 476–488 (2006)
6. C.H. Chang, E.I. Franses, Modified Langmuir–Hinshelwood kinetics for dynamic adsorption of surfactants at the air/water interface. *Colloids Surf.* **69**, 189–201 (1992)
7. P.G. Ciarlet, Basic error estimates for elliptic problems, in *Handbook of Numerical Analysis*, vol. II, ed. by P.G. Ciarlet, J.L. Lions (North-Holland, Amsterdam, 1993), pp. 17–351
8. Z. Denkowski, S. Migórski, N.S. Papageorgiou, *An Introduction to Nonlinear Analysis: Theory* (Kluwer Academic/Plenum Publishers, Boston, 2003)
9. G. Dziuk, C.M. Elliott, Surface finite elements for parabolic equations. *J. Comput. Math.* **25**, 385–407 (2007)
10. J.R. Fernández, P. Kalita, S. Migórski, M.C. Muñoz, C. Núñez, Variational analysis of the Langmuir–Hinshelwood dynamic mixed-kinetic adsorption model. *Nonlinear Anal. Real World Appl.* **15**, 205–220 (2014)
11. J.R. Fernández, P. Kalita, S. Migórski, M.C. Muñoz, C. Núñez, Existence and uniqueness results for a kinetic model in bulk-surface surfactant dynamics. *SIAM J. Math. Anal.* **48**(5), 3065–3089 (2016)
12. J.R. Fernández, M.C. Muñoz, Numerical analysis of surfactant dynamics at air-water interface using the Henry isotherm. *J. Math. Chem.* **49**, 1624–1645 (2011)
13. J.R. Fernández, M.C. Muñoz, C. Núñez, A mixed kinetic-diffusion surfactant model for the Henry isotherm. *J. Math. Anal. Appl.* **389**, 670–684 (2012)
14. D. Gilbarg, N.S. Trudinger, *Elliptic Partial Differential Equations of Second Order* (Springer, Berlin, 1983)
15. F. Hecht, New development in FreeFem++. *J. Numer. Math.* **20**(3–4), 251–265 (2012)
16. P. Joos, G. Serrien, Adsorption kinetics of lower alkanols at the air/water interface: effect of structure makers and structure breakers. *J. Colloid Interface Sci.* **127**, 97–103 (1989)
17. S. Khatri, A.K. Tornberg, A numerical method for two phase flows with insoluble surfactants. *Comput Fluids* **49**, 150–165 (2011)
18. J.M. Lee, *Introduction to Smooth Manifolds* (Springer, Berlin, 2013)
19. I.L. Novak, F. Gao, Y.S. Choi, D. Resasco, J.C. Schaff, B.M. Slepchenko, Diffusion on a curved surface coupled to diffusion in the volume: application to cell biology. *J. Comput. Phys.* **226**, 1271–1290 (2007)
20. R.E. Showalter, *Monotone Operators in Banach Space and Nonlinear Partial Differential Equations* (American Mathematical Society, Providence, 1997)
21. J. Wloka, *Partial Differential Equations* (Cambridge University Press, London, 1987)